

PAPER • OPEN ACCESS

Kinematic and thermodynamic operational analysis of rhombic-drive Stirling engine prototype

To cite this article: Mohd Farid Zainudin *et al* 2020 *IOP Conf. Ser.: Mater. Sci. Eng.* **788** 012070

View the [article online](#) for updates and enhancements.

You may also like

- [Manufacturing and testing prototype of a gamma type Stirling engine for micro-CHP application](#)
Jufrizal, Farel H. Napitupulu, Ilmi *et al.*
- [Effects of phase angle setting, displacement, and eccentricity ratio based on determination of rhombic-drive primary geometrical parameters in beta-configuration Stirling engine](#)
Z M Farid, A B Rosli and K Kumaran
- [Experimental and numerical analysis of a liquid-piston Stirling engine with multiple unit sections](#)
S. Tamura, H. Hyodo and T. Biwa



The Electrochemical Society
Advancing solid state & electrochemical science & technology

243rd ECS Meeting with SOFC-XVIII

More than 50 symposia are available!

Present your research and accelerate science

Boston, MA • May 28 – June 2, 2023

[Learn more and submit!](#)

Kinematic and thermodynamic operational analysis of rhombic-drive Stirling engine prototype

Mohd Farid Zainudin¹, Rosli Abu Bakar^{1,*}, Kumaran a/l Kadirgama¹ and Gan Leong Ming¹

¹ Faculty of Mechanical & Manufacturing Engineering, Universiti Malaysia Pahang, 26600 Pekan, Pahang, Malaysia.

*corresponding author: rosli@ump.edu.my

Abstract. This operational analysis is aimed for the next development of rhombic-drive beta-configuration Stirling engine prototype. The kinematic analysis focused on the adjustment of crank radius and connecting rod length, for achieving optimum phase angle setting and suitable eccentricity ratio based on geometrical constraints. The isothermal thermodynamic analysis is carried out to predict the engine performance between the baseline and proposed design parameters. The reciprocating displacement of moving pistons, volumetric displacement, cyclic pressure, energy produced and thermal efficiency are derived and solved. The results show that the reduction of crank radius increases the eccentricity ratio, while both reduction of connecting rod length and crank radius increase the phase angle setting. It is found that as the phase angle setting increase, the engine power output and thermal efficiency increase. The magnitudes of engine power and thermal efficiency may be elevated by modifying the geometrical design and operating condition.

Keyword. Stirling engine, rhombic-drive, kinematic, thermodynamic, phase angle setting.

1. Introduction

In the current situation, the interest in alternative energy sources and effective energy conversion systems has significantly increased. Although fossil fuels meet the most of the world's energy demand, the continuous usage would lead to rapid depletion, climate change and worsening environmental issues [1, 2]. Among the possible alternative solutions to address present energy and environmental problems, Stirling engines have attracted significant attention in recent years due to their advantages of high thermal efficiency, low maintenance requirement, and flexibility on the usage of energy sources with low emissions level [3]. Stirling engines are an externally-heated engine, operate with a closed thermodynamic cycle contained with several gases as working fluid. Several energy sources such as combustible materials, solar radiation, geothermal, or any waste heat dissipation can be used to power the engine [4].

Stirling engines are generally classified in two categories; kinematic and free-piston engines. In free-piston engines, piston and displacer synchronization is provided by springs and gas pressure [1]. Kinematic engines consists of a driving mechanism such as crank-drive, rhombic-drive, lever-drive, ross-yoke drive, swash-plate drive, wobble-plate drive and scotch-yoke drive [5-9]. According to cylinder configurations, Stirling engines can be classified in three types; alpha-, beta- and gamma-



configuration. In alpha engine, both cylinders contain a piston, while gamma engine contains a power piston and displacer. Beta engine has one cylinder and both displacer and power piston are placed coaxially in the same cylinder [10].

In the past decades, the studies about Stirling engines were performed, and the main research were conducted on manufacturing, testing and further development [1, 2, 11-13]. However, in the development of Stirling engine working prototype, it was found that the major challenges are the time consuming in the design process and the cost of fabrication. There is a limitation in the determination of geometrical parameters of the engine based on technical experience and insufficient costly experimental information. The improvement of the engine design is carried out in a relatively high cost and time consuming, and also involving trial-and-error process. Therefore, a number of numerical models and simulation methods had been introduced and discussed in order to decrease the development cost and time consuming [14]. However, the design and operating validation on the practical working prototype is needed based on the actual working condition.

The development of rhombic-drive working prototype with small volumetric displacement is available and the research is still continuing for enhancing the engine performance. For Dish-Stirling system, single cylinder with enormous piston and displacer design sizes are less effective, which can leads to higher inertia force and heat transfer rate. In comparison with conventional reciprocating engines, rhombic-drive mechanism does not require a crankshaft. For multi-cylinder arrangement, the cylinders intergration without over-sizing the geometrical parameters indicate significant challenge for Dish-Stirling system development [18]. Based on the previous development of Dish-Stirling system proposed by [18], further prototype investigation and analysis are being carried out. This work is performed as a preliminary study for the next engine development. The objective of this work is to determine the suitable engine geometrical parameters and perform a comparative discussion between existing and proposed design parameters.

2. Methodology

The determination of geometrical parameters for driving mechanism is crucial for achieving power output and efficiency, as well as ensuring successful engine operation. Various aspects have to be considered; design compactness, components inertia, operating conditions, allowable clearance and tolerance, etc. within the stage of the Stirling engine development. In this paper, a comparative kinematic investigations of rhombic-drive geometrical parameters between previous and proposed design parameters will be presented and discussed. For the Stirling engine prototype analysis, two scopes will be discussed, namely kinematic analysis and thermodynamic cycle prediction.

2.1. Kinematic operation based on phase angle setting

Phase angle setting plays an important role in enhancing the Stirling engine power output and thermal efficiency. Lower phase angle setting causing shorter heat transfer period for the contained working fluid to absorb the heat from the heat source and contract through the cooling source [18]. For phase angle setting determination, the top dead center (TDC) and bottom dead center (BDC) crank angle position for both displacer and power piston are needed [15]. Figure 1 shows the schematic diagram for the determination of TDC and BDC crank angle position for both displacer and power piston. The TDC position of power piston is defined as the crank offset, r and connecting rod, L_p are in one straight line (figure 1 (a)) and the TDC position of displacer is determined when the connecting rod, L_d and crank offset, r are in collinear to each other (figure 1 (b)).

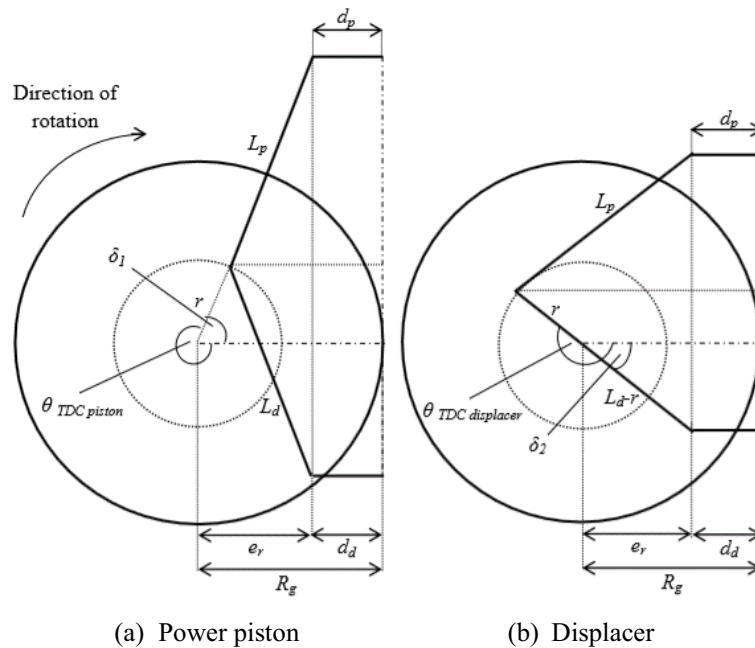


Figure 1. Schematic diagram for TDC crank angle position for power piston and displacement.

The phase angle is determined by calculating the difference of TDC position for both displacer and power piston. The calculation starts by determining the crank angle, θ for both displacer and power piston TDC position. From the calculation, the difference crank angle TDC position between displacer and power piston can be determined, since the displacer leads the power piston movement [15]. Considering the horizontal line as the crank angle's reference axis, the crank angle TDC position for both displacer and power piston can be calculated by using the following equation (1) and (2):

$$\theta_{TDC\ piston} = 360^\circ - \left[\cos^{-1} \left[\frac{R_g - d_p}{r + L_p} \right] \right] \quad (1)$$

$$\theta_{TDC\ displacer} = 180^\circ + \left[\cos^{-1} \left[\frac{R_g - d_d}{L_d - r} \right] \right] \quad (2)$$

The phase angle setting can be determined by calculating the difference between TDC position for both displacer and power piston, which is using the following equation (3):

$$\alpha = \theta_{TDC\ piston} - \theta_{TDC\ displacer} \quad (3)$$

2.2. Determination of engine displacement

The determination of engine displacement, S can be performed based on the variations of rhombic-drive geometrical parameters. Based on the principle of rhomboid, the displacement for both displacer and power piston can be described as equal, due to the symmetrical configuration at vertical axis, as illustrated in figure 1. The engine displacement can be determined by using equation (4)[15]:

$$S = \frac{r}{\lambda} \left[\left((1 + \lambda)^2 - (\lambda^2 \varepsilon^2) \right)^{1/2} - \left((1 - \lambda)^2 - (\lambda^2 \varepsilon^2) \right)^{1/2} \right] \quad (4)$$

where the eccentricity ratio, ε

$$\varepsilon = \frac{e}{r}, \varepsilon > 1 \quad (5)$$

$$\lambda = \frac{r}{L} (e + r) < L \quad (6)$$

2.3. Thermodynamic cycle prediction

A schematic diagram of the beta-configuration Stirling engine is shown in figure 2. The applied model has been divided into three control volumes: (1) expansion chamber, (2) regenerative channel, (3) compression chamber, based on the numerical model presented by [16]. It is assumed that the working fluid is an ideal gas and the volumes of the chambers as well as the pressures, temperatures and masses of the air in the expansion and the compression chambers are varying with respect to the crank angle position. For the proposed design parameters, similar methodology approach is applied to the working space of the engine. It is assumed that there are no internal heat exchanger surfaces, but only depends on the displacer and power piston cylinder walls for heat addition and rejection process.

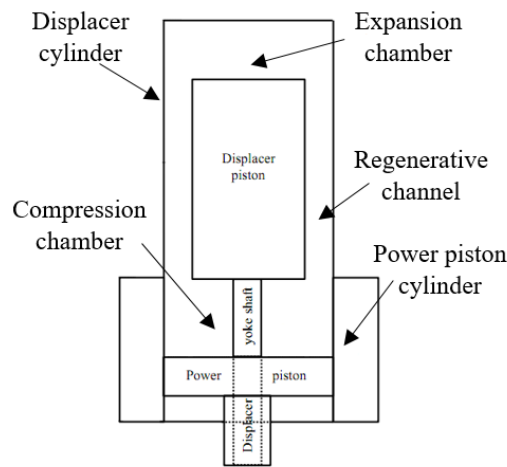


Figure 2. Schematic diagram of beta-configuration engine.

Figure 3 shows the schematic diagram for rhombic-drive beta-configuration Stirling engine. For this configuration, it is assumed that the expansion chamber consists of the expansion space clearance and displacer swept volume. For regenerative channel, it is assumed that regenerating process occurs between the displacer-cylinder gap, as the consideration of minimum dead volume. Meanwhile, the compression chamber consists of clearance and displacer lower surface-piston swept volume.

The expansion chamber varies over a cycle with the movement of the displacer piston, while the compression chamber varies based on the movement of both lower displacer and power piston. In rhombic-drive mechanism, two units of equal spur gears are meshed together and rotate opposite to each other. Four units of identical connecting rods, displacer and power piston yoke, are used to provide reciprocating motion with minimum side thrust for both displacer and power pistons. The reciprocating displacement of both displacer, Y_d and power piston, Y_p that connected to the rhombic-drive mechanism can be calculated by using following equation (7) and (8) [16]:

$$Y_d = L_{dt} + r \sin \theta - [L^2 - (R_g - d_d - r \cos \theta)^2]^{1/2} \tag{7}$$

$$Y_p = L_{pt} + r \sin \theta + [L^2 - (R_g - d_p - r \cos \theta)^2]^{1/2} \tag{8}$$

where the crank angle, θ is rotating in a clockwise direction. The reciprocating volumetric displacement of expansion chamber, V_e and compression chamber, V_c can be determined based on Y_d and Y_p . Considering the cross-sectional area of displacer and power piston, the displacement volume of V_e and V_c can be expressed as (9) and (10):

$$V_e = \pi(b_d^2/4) (L_t - Y_d) \tag{9}$$

$$V_c = \pi(b_p^2/4) (Y_p + (Y_d - l_d)) \tag{10}$$

Based on ideal-gas equation of state, the pressure in the expansion and compression chambers are calculated by (11) and (12):

$$P_e = \frac{m_e RT_e}{V_e} \tag{11}$$

$$P_c = \frac{m_c RT_c}{V_c} \tag{12}$$

where m_e and m_c are the mass and T_e is the temperature of the air contained in the expansion chamber, T_c is the sink ambient temperature and R is the gas constant.

For design performance evaluation, an ideal isothermal model based on Schmidt theory is adopted [18]. The classic Stirling cycle analysis provide a basic understanding for an ideal condition for the engine operation. The approach presented by Schmidt for the thermodynamic analysis based on ideal isothermal model derived the pressure relation by the equation (13) [18]:

$$P = MR \left(\frac{V_c}{T_c} + \frac{V_k}{T_c} + \frac{V_r \ln(T_h/T_c)}{T_h - T_c} + \frac{V_h}{T_h} + \frac{V_e}{T_h} \right)^{-1} \tag{13}$$

The compression work done, W_c , and expansion work, W_e , can be calculated by using the following equation (14) and (15):

$$W_c = \pi V_{swc} P_{mean} \sin \beta (\sqrt{1 - b^2} - 1) / b \tag{14}$$

$$W_e = \pi V_{swe} P_{mean} \sin(\beta - \alpha) (\sqrt{1 - b^2} - 1) / b \tag{15}$$

Since the Schmidt analysis is based on ideal isothermal model, the thermal efficiency is defined by the ratio of the work done by the engine to the heat supplied externally to the engine, thus the thermal efficiency, (16):

$$\eta = \frac{W_{net}}{W_e} = \frac{W_e + W_c}{W_e} \tag{16}$$

The overall design parameters will be determined based on rhombic-drive features with compensation between engine displacement, phase angle setting, components tolerance and failure factors. The design parameters based on previous engine design developed by [18] is summarized in table 1.

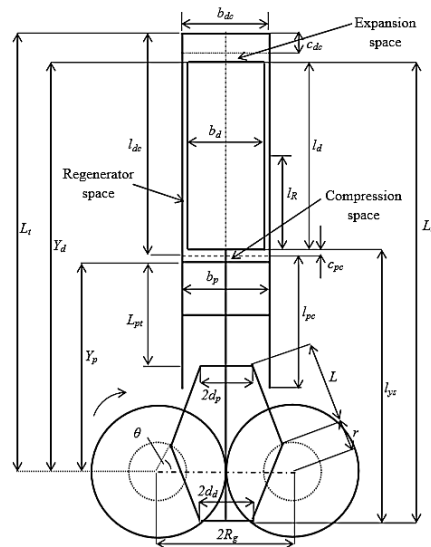


Figure 3. Schematic diagram for rhombic-drive.

Table 1. Design parameters proposed by [18].

Components	Label	Dimension (mm)
Total length	L_t	473
Displacer cylinder length	l_{dc}	175
Displacer cylinder bore	b_{dc}	84
Displacer top clearance	c_{dc}	3
Displacer length	l_d	180
Displacer diameter	b_d	81
Regenerator length	l_R	29
Piston top clearance	c_{pc}	3
Piston length	L_{pt}	99
Piston cylinder length	l_{pc}	160
Piston cylinder bore	b_p	80
Yoke shaft	l_{ys}	362
Piston yoke	$2d_p$	50
Displacer yoke	$2d_d$	50
Connecting rod	L	120
Crank offset	r	38
Spur gear PCD	$2R_g$	130

3. Results and discussion

Based on the previous design parameters proposed by [18], the TDC and BDC crank angle position for both displacer and power piston, and the phase angle are summarized in table 2, based on the equations (1) to (3). The crank angle position for TDC and BDC for both displacer and power piston are determined based on reference TDC crank angle position for power piston. According to [19], 90° phase angle setting indicates the optimum arrangement for Stirling engine for achieving high power output, due to high expansion and heat transfer between hot and cold spaces, as shown in figure 4. However, for this arrangement, after compensating the components operation, tolerance and maintenance constraint, the displacer moved about 44° ahead during the engine cycle, leading the power piston to transfer the working gas between the expansion and compression spaces for heating and cooling processes.

Table 2. TDC and BDC position for displacer and power piston with phase angle setting.

	Crank angle, θ ($^\circ$)	
	TDC	BDC
Displacer	240.80	75.34
Power piston	284.66	119.20
Phase angle, α	44	

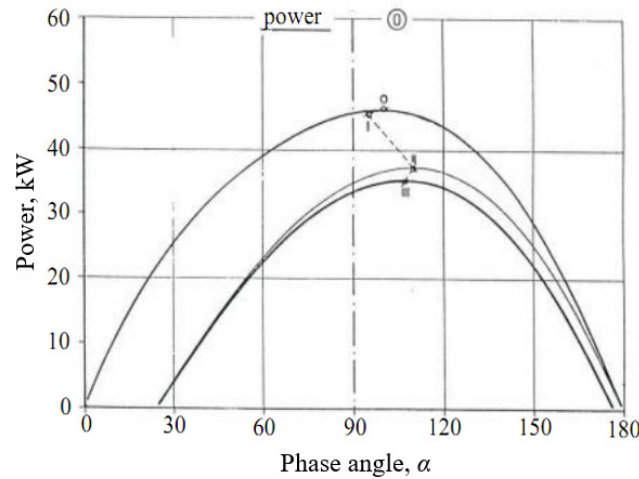


Figure 4. Effect of phase angle setting in Stirling engine [19].

Based on the 44° phase angle setting, the reciprocating displacement for both displacer and power piston are shown in figure 5. For rhombic-drive mechanism, the displacer and power piston will move downward at the same time, in the crank interval from 20° to 120° crank angle. At this particular range, the distance between displacer lower and piston top surfaces indicate the presence of dead volume during the engine cycle. Based on the previous design parameters, the significant distance between displacer lower and piston top surface indicate a significant amount of dead volume. According to [16], less minimum distance means smaller dead volume in the compression space, and more working fluid in the compression space is being drawn into the expansion space for heating, while providing a clearance as long as the displacer and power piston do not coincide with each other.

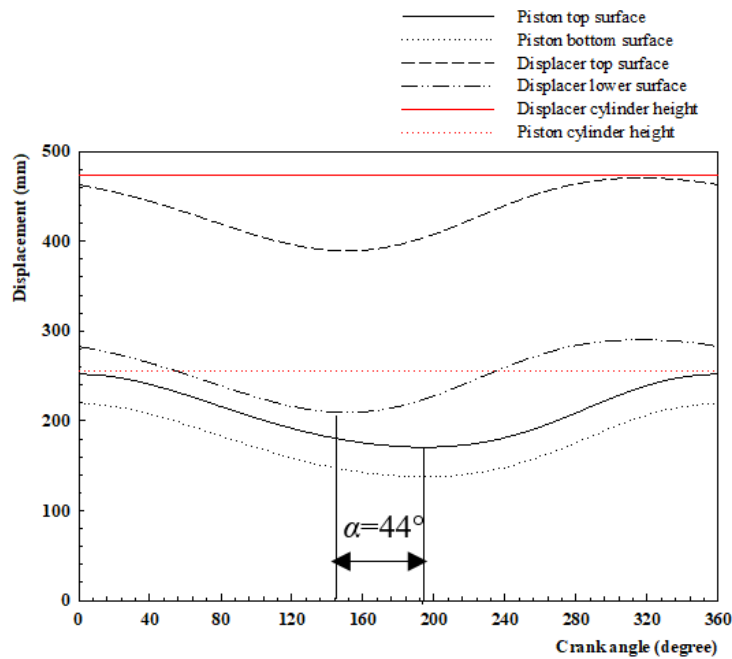


Figure 5. Displacement plot based on parameters in [18].

The volumetric displacement of rhombic-drive mechanism for 44° phase angle setting is shown in figure 6. The swept volume for expansion and compression space with respect to the crank angle is determined by using the equation (9) and (10). Meanwhile, the dead volumes for clearance, heater, regenerator and cooler space remain constant, fully determined based on the design geometrical parameters. Based on the reciprocating displacement plot in figure 5, as the displacer and power piston moving downwards, the volume in the expansion space increase while the volume in the compression space remain almost constant with a significant value, since the design has internal regenerator configuration, as shown in figure 7. At 140° crank angle, the volume in the expansion space reaches its maximum and starts to decrease while the compression space volume increase. Within the crank angle from 240 to 280°, the compression space volume reach to its maximum and the volume in the expansion space reach to its minimum at 320°. Based on this phase angle setting, the design induced higher heating period for the working fluid to absorb the thermal energy from the heat source, as the working fluid flows to the expansion space. However, the design indicates shorter cooling period for the heater working fluid to be rejected to the cooler when it flows to the compression space.

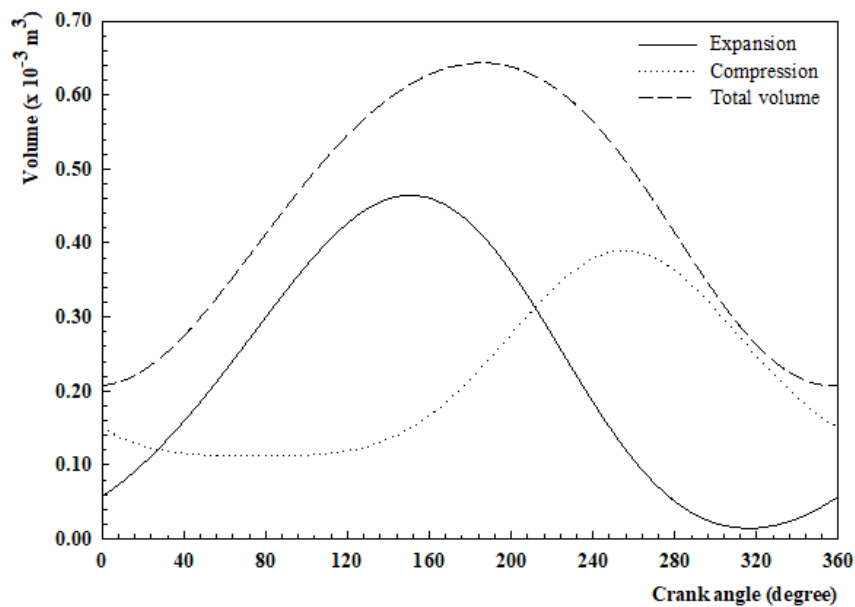


Figure 6. Volumetric displacement of 44° phase angle setting.

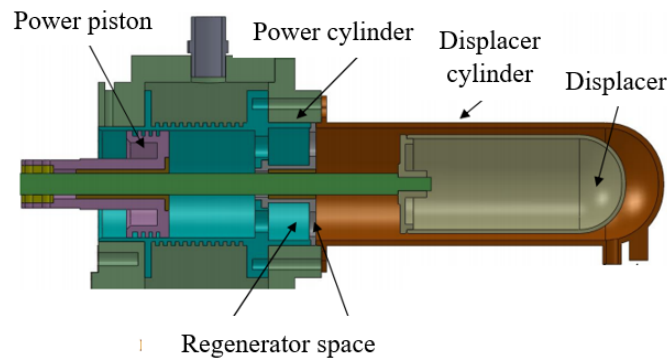


Figure 7. Displacer and power piston cylinder design [18].

The P-V plot for previous design parameters is shown in figure 8. The area of the total volume indicates the output from the design. Based on the Schmidt ideal isothermal analysis, it is assumed that the design has a perfect regeneration, the expansion and compression process are isothermal, there is no leakage of working fluid mass, and the working fluid obeys the ideal gas law. The performance of the engine is summarized in table 3. It is noticed that the engine produce power of 105 Watt at 2000 rpm, based on the operating variables, $T_h = 800$ K, $T_c = 300$ K, 44° phase angle setting and operates at atmospheric pressure condition, which are the operating variables in numerical analysis carried out by [16]. The thermal efficiency of the thermodynamic cycle reaches merely 27%, which is quite low since the engine operates on atmospheric condition, and moderate heating temperature. However, the magnitudes of the engine power output and thermal efficiency may be varying by modifying the geometrical design or by adding and increasing the regeneration effectiveness of the regenerative channel [16].

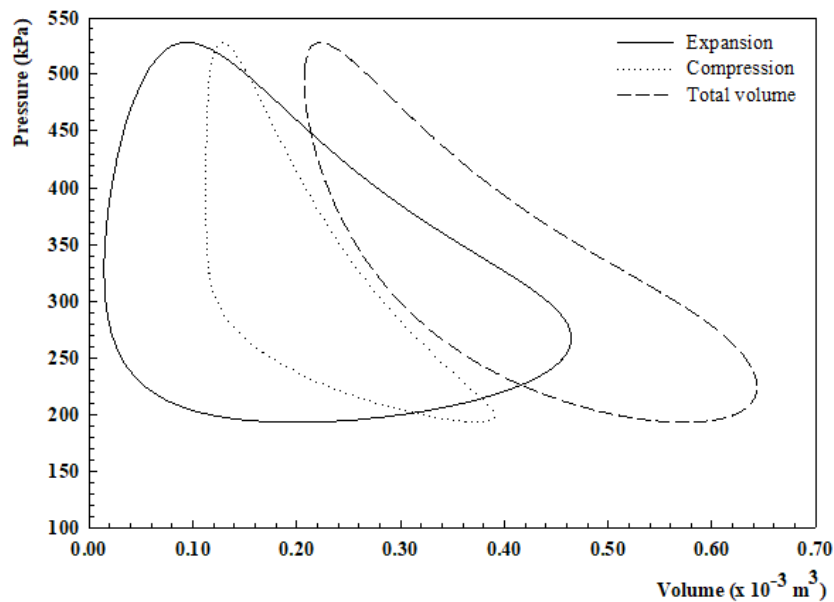


Figure 8. P-V diagram for 44° phase angle setting.

Table 3. Performance output based on ideal isothermal analysis.

Output	Value	
	Expansion	Compression
Working space (Joule/cycle)	11.988	-8.838
Total energy (Joule/cycle)	3.150	
Thermal efficiency (%)	26.28	
Power at 2000 rpm (Watt)	105	
Expansion temperature (K)	800	
Compression temperature(K)	300	

Figure 9 shows the pressure variation inside the expansion and compression chambers during the engine cycle. The pressure varied periodically, and the pressure difference between those chambers are indicated as a driving forces to make the working fluid moves back and forth between the expansion

and compression chambers. It is noticed that higher pressure developed as the power piston reached at TDC position, which inducing minimum volume at expansion chamber. At this condition, most of the working fluid is being transferred to the expansion chamber to be heated, while lower pressure developed as the power piston reached its BDC position, as the working fluid is being transferred to the compression chamber to be cooled.

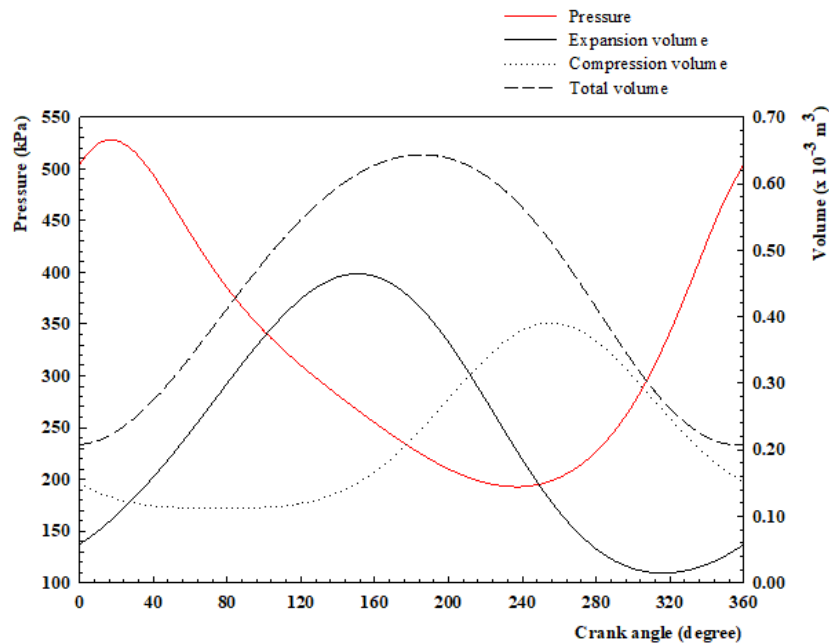


Figure 9. Pressure-volume variation based on parameters in [18].

For the next development stage of rhombic-drive beta-configuration Stirling engine, a few new design parameters are being considered in order to enhance the engine performance, with consideration of operational characteristics of rhombic-drive mechanism itself, and also to ensure a proper functionality and to avoid any mechanism failures. For rhombic-drive mechanism, the eccentricity ratio, ε usually lies between $1 < \varepsilon < 2$ in order to avoid any jerky motion of links and excessive vibrations. It can be controlled by suitably selecting the crank radius, eccentricity ratio, and connecting rod length [15]. Therefore, the new design parameters will be proposed with taking into account the adjustment of crank offset radius and connecting rod length. Based on the preliminary study on the effects of crank radius, connecting rod length to the phase angle setting and eccentricity ratio performed by [20], the new proposed design parameters are listed in table 4.

Table 4. Proposed design parameters.

Parameters	[18]	Proposed
Crank offset radius, r (mm)	38	30
Connecting rod length, L (mm)	120	80.5
Phase angle, α ($^\circ$)	43.90	73.60
Stroke, S (mm)	81.20	72.17
Eccentricity ratio, ε	1.05	1.33

Based on the previous preliminary study in [20], it was found that the variation of crank offset radius has significant effect to the eccentricity ratio, however reflecting a small change in engine phase angle. For the next development stage, the crank offset radius is reduced up to 21% from the original design, which gives the new radius of 30mm and 1.33 for the eccentricity ratio. Meanwhile, the connecting rod length is reduced up to 33% from the original length, which gives the new connecting rod length of 80.5mm in order to reach almost 74° of phase angle setting. Since there is a change in crank offset radius and connecting rod length, the engine stroke is decreased from 81.20mm to 72.17mm. Based on the changes in parameters listed in table 3, several adjustments for other design parameters also need to be considered while taking into account which consists of minimum dead volume, components clearance space, minimum modification work, geometrical constraints, and avoiding any mechanical failures. Meanwhile, table shows a comparison of TDC and BDC position for both displacer and power piston between the previous and proposed design parameters.

Table 5. Comparison of TDC and BDC between previous and proposed design.

	Crank angle, θ ($^\circ$)			
	Ming (2012)		Proposed	
	TDC	BDC	TDC	BDC
Displacer	240.80	75.34	217.62	68.78
Power piston	284.66	119.20	291.22	142.38
Phase angle, α	43.90		73.60	

Based on the new proposed design parameters, the reciprocating displacement for both displacer and power piston are shown in figure 10. During the engine cycle, the displacer moves at 74° phase angle ahead of the power piston to draw the working fluid traversing back and forth between the expansion and compression spaces for heating and cooling processes. At some instants, the displacer and power piston were closed to each other, with the crank interval from 40 to 100° crank angle. Within this range, the minimum distance between the displacer lower and power piston top surfaces are treated to be influential factors that affect the dead volume of the engine. In comparison with previous design, the proposed design parameters indicate lower dead volume in the compression space, as a result inducing more working fluid is being drawn to the expansion space for heating. It can be noticed that the phase angle setting has a significant effect to the adjustment of dead volume. The adjustment of crank radius and connecting rod length in rhombic-drive mechanism allows minimum dead volume control, which affecting the engine performance [17].

The volumetric displacement of rhombic-drive mechanism for 74° phase angle setting is shown in figure 11. In comparison of original design, there is no significant difference in volumetric displacements trend. Based on the reciprocating displacement plot in figure 10, as the displacer and power piston moving downwards, the volume in the expansion space increase while the volume in the compression space remain almost constant within the crank interval from 40 to 100° . At 140° crank angle, the volume in the expansion space reaches its maximum and starts to decrease while the compression space volume increase. Within the crank angle from 240 to 260° , the compression space volume reach to its maximum and the volume in the expansion space reach to its minimum at 280° . Based on the proposed phase angle setting, higher working fluid mass is drawn to the expansion space during heating process, since minimum dead volume presence in compression space. After the heating process, the working fluid is drawn to the compression space. Based on this condition, the proposed design parameters induced higher expansion rate for the working fluid to absorb the thermal energy from the heat source, as higher working fluid flows to the expansion space. Similarly, the design also indicates better compression and cooling process, as most of the heated working fluid mass is released to the cooler when it flows to the compression space.

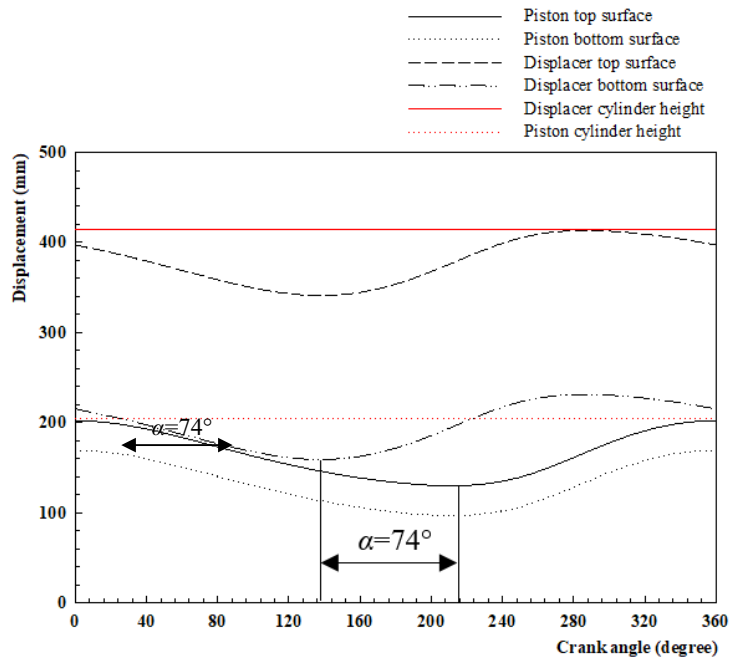


Figure 10. Displacement plot for proposed design parameters.

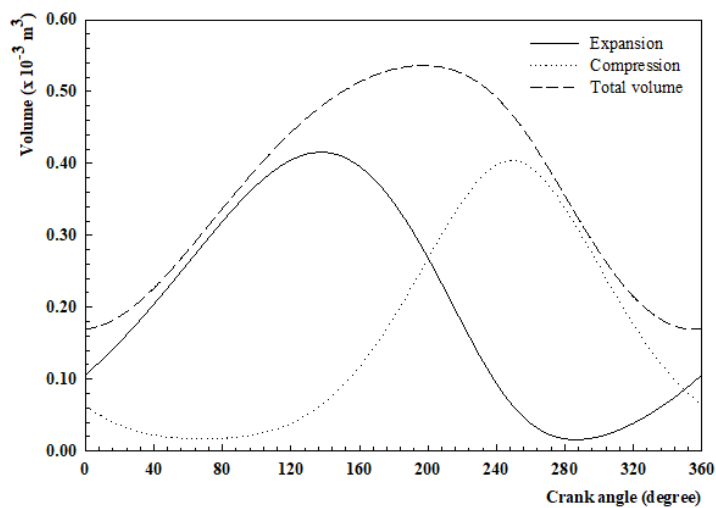
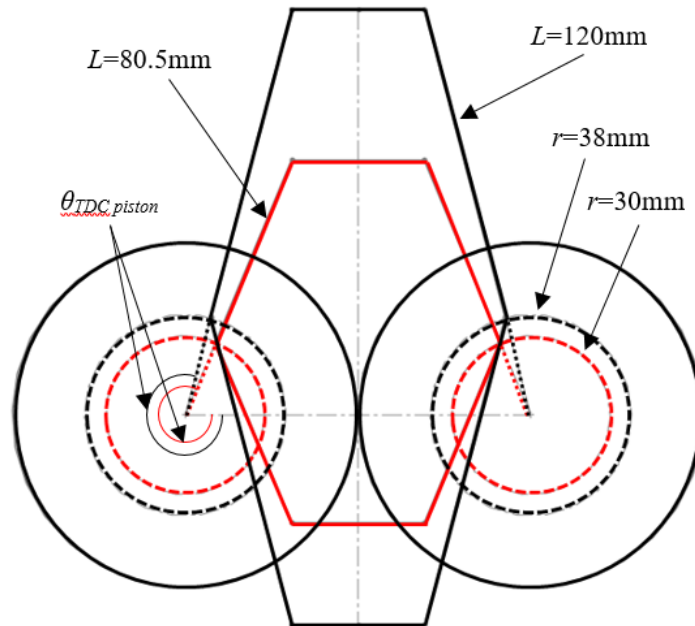
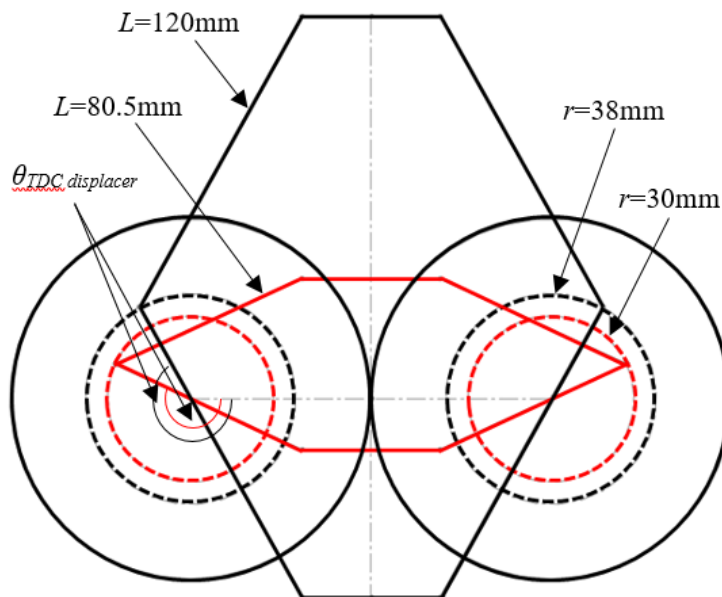


Figure 11. Volumetric displacement for 74° phase angle setting.

Figure 12 illustrates the comparison of displacer and power piston at TDC position based on different crank radius and connecting rod length. Based on the comparison of TDC position in table 4 and figure 8, there is only slight difference in power piston TDC of crank angle position, however induced significant changes in displacer TDC crank angle position, for different crank radius and connecting rod length. Based on this condition, the significant distance between displacer and piston yoke indicate that the working fluid is displaced at maximum displacement volume to the cooling space, while the cooled working fluid is moved to the expansion space at maximum volume.



(a) Schematic diagram for power piston TDC position.



(b) Schematic diagram for displacer TDC position.

Figure 12. Comparison of TDC for both displacer and power piston at different r and L .

Figure 13 shows the P-V diagram for 74° phase angle setting. Fig. 14 shows the comparison of cyclic pressure and P-V diagram based on 44° and 74° phase angle setting. The proposed design indicates higher cyclic pressure within the crank angle interval 0 - 40°. The proposed design parameters induced higher cyclic pressure, as the adjustment of crank radius and connecting rod length reduces the compression space dead volume. In the crank interval from 240 - 280°, similar cyclic pressure is found for both designs, since there is no significant difference in power piston TDC as the crank radius and connecting rod length reduced.

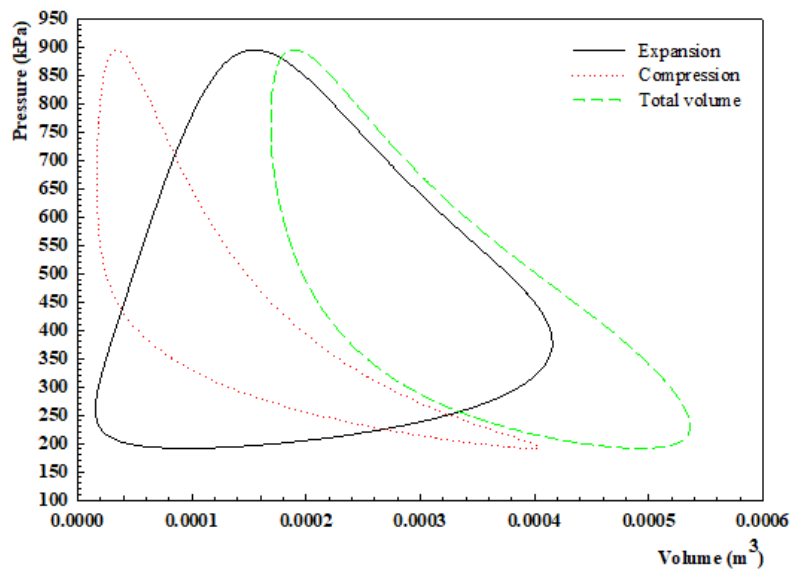
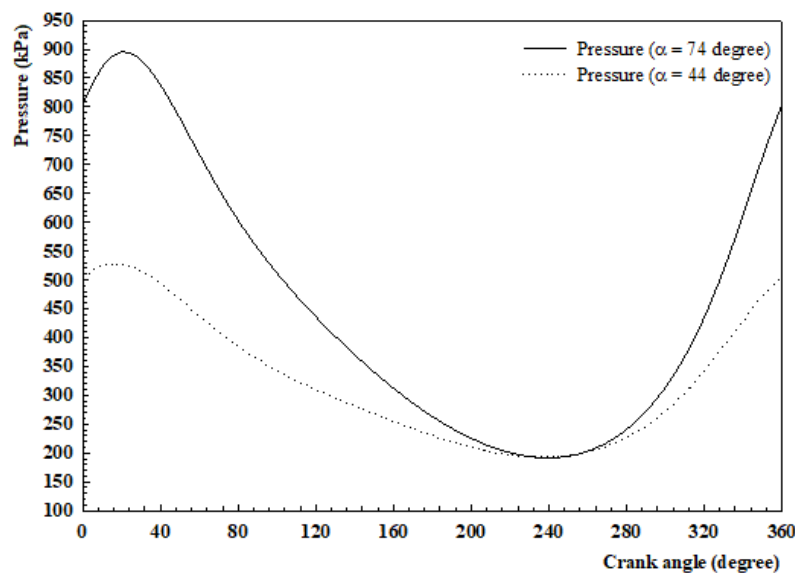
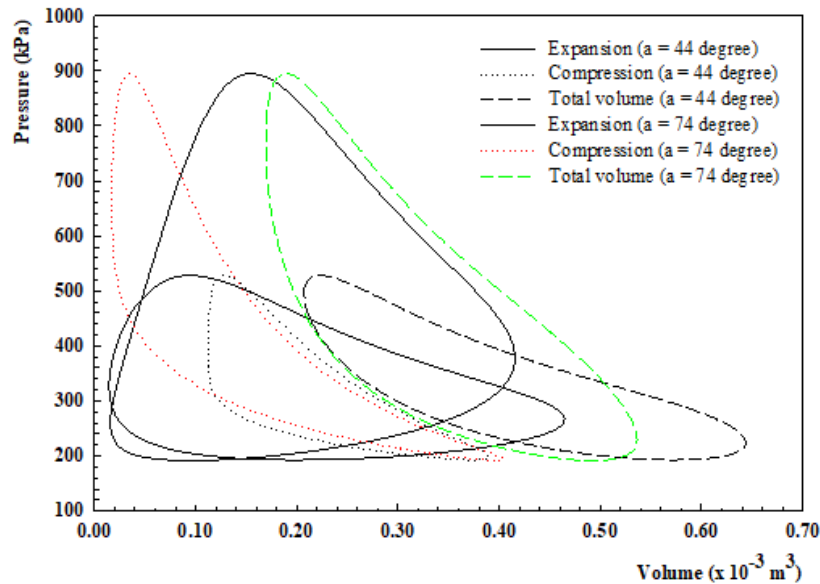


Figure 13. P-V diagram for 74° phase angle setting.



(a) Cyclic pressure.



(b) P-V diagram.

Figure 14. Comparison of cyclic pressure and P-V diagram.

Table 6 summarized the comparison of engine performance between the numerical model prediction carried out by [16], prototype developed by [18] and proposed design parameters in the present work. Based on same heat source and cooling source temperature, engine speed, and operates at atmospheric pressure, it is noticed that the power output and thermal efficiency for proposed design parameters increased, in comparison with previous design in [18]. For numerical model prediction based on parameters in [16], it is noticed that the performance is frequently encountered with the small-scale engines. However, the magnitudes of the engine power and thermal efficiency may be elevated by modifying the geometrical design.

Table 6. Comparison of engine performance.

Output	[16]	[18]	Proposed design
Expansion work (Joule/cycle)	3.791	11.988	12.322
Compression work (Joule/cycle)	-3.288	-8.838	-8.737
Total energy (Joule/cycle)	0.503	3.150	3.584
Thermal efficiency (%)	13.10	26.28	29.10
Power (Watt)	16.75	105	119

4. Conclusion

The kinematic and thermodynamic operational analysis of Stirling engine with rhombic-drive mechanism based on ideal isothermal analysis has been carried out in the present work. The reciprocating displacement of displacer and power piston assembly, volumetric displacement of expansion, compression and total volumes, the prediction of cyclic pressure, expansion and compression work, power output and thermal efficiency based on different crank radius and connecting rod length effects to the engine performance are been presented and discussed.

Results show that by adjusting the influential design geometrical parameters in rhombic-drive mechanism, such as crank radius and connecting rod length, and proper selection of eccentricity ratio, ε , higher phase angle setting and cyclic pressure can be achieved, thus increasing the engine power output and thermal efficiency. Regardless of adjustments to the other geometrical parameters, the reduction of crank radius, r and connecting rod length, L leads to higher phase angle, α , which induced by the difference of TDC crank angle position for both displacer and power piston, however minor changes to the engine stroke, S .

The power output and thermal efficiency of the previous design is predicted to produce 105 W and 26.28% at 2000 rpm, based on $r=38\text{mm}$, $L=120\text{mm}$, and $\alpha=44^\circ$. Based on the adjustment of crank radius, r from 38 to 30mm and connecting rod length, L from 120 to 80.5mm, the phase angle setting, $\alpha=74^\circ$, the power output increase to 119 W, accompanied by the thermal efficiency of 29.10%. It is observed that the adjustment of phase angle setting contributes affecting the engine performance, which increasing the power output and thermal efficiency.

Acknowledgement

The authors would like to thank the Ministry of Higher Education for their financial support under Grant RDU 190159, and thank to Universiti Malaysia Pahang for providing the facilities for the engine development.

References

- [1] Cinar C, Aksoy F, Solmaz H, Yilmaz E and Uyumaz A 2018 Manufacturing and testing of an alpha Stirling engine *Applied Thermal Engineering* **130** 1373-9
- [2] Karabulut H, Yücesu H S, Çınar C and Aksoy F 2009 An experimental study on the development of a β -type Stirling engine for low and moderate temperature heat sources *Applied Energy* **86** 68-73
- [3] Chen W-L, Wong K-L and Chen H-E 2014 An experimental study on the performance of the moving regenerator for a gamma-type twin power piston stirling engine *Energy Conversion and Management* **77** 118-28
- [4] Cinar C and Karabulut H 2005 Manufacturing and testing of gamma type Stirling engine *Renewable Energy* **30** 57-66
- [5] Erol D, Yaman H and Doğan B 2017 A review development of rhombic drive mechanism used in the Stirling engines *Renewable and Sustainable Energy Reviews* **78** 1044-67
- [6] Aksoy F, Karabulut H, Cinar C, Solmaz H, Ozgoren Y O and Uyumaz A 2015 Thermal performance of a Stirling engine powered by a solar simulator *Applied Thermal Engineering* **86** 161-7
- [7] Solmaz H and Karabulut H 2014 Performance comparison of a novel configuration of beta-type Stirling engines with rhombic drive engine *Energy Conversion and Management* **78** 627-33
- [8] Karabulut H, Aksoy F and Oztürk E 2009 Thermodynamic analysis of a beta-type Stirling engine with a displacer driving mechanism by means of a lever *Renewable Energy* **34** 202-8
- [9] Thombare D G and Verma S K 2008 Technological development in the Stirling cycle engines *Renewable and Sustainable Energy Reviews* **12** 1-38
- [10] Hachem H, Gheith R, Aloui F and Ben Nasrallah S 2018 Technological challenges and optimization efforts of the Stirling machine: A review *Energy Conversion and Management* **171** 1365-87
- [11] Cinar C, Yucesu S, Topgul T and Okur M 2005 Beta-type Stirling engine operating at atmospheric pressure *Applied Energy* **81** 351-7
- [12] Cheng C-H, Yang H-S and Keong L 2013 Theoretical and experimental study of a 300 W beta-type Stirling engine *Energy* **59** 590-9
- [13] Li T, Tang D, Li Z, Du J, Zhou T and Jia Y 2012 Development and test of a Stirling engine driven by waste gases for the micro-CHP system *Applied thermal engineering* **33** 119-23
- [14] Ahmadi M H, Ahmadi M-A and Pourfayaz F 2017 Thermal models for analysis of performance

- of Stirling engine: A review *Renewable and Sustainable Energy Reviews* **68** 168-84
- [15] Shendage D J, Kedare S B and Bapat S L 2011 An analysis of beta type Stirling engine with rhombic drive mechanism *Renewable Energy* **36** 289-97
- [16] Cheng C-H and Yu Y-J 2010 Numerical model for predicting thermodynamic cycle and thermal efficiency of a beta-type Stirling engine with rhombic-drive mechanism *Renewable Energy* **35** 2590-601
- [17] Kongtragool B and Wongwises S 2006 Thermodynamic analysis of a Stirling engine including dead volumes of hot space, cold space and regenerator *Renewable Energy* **31** 345-59